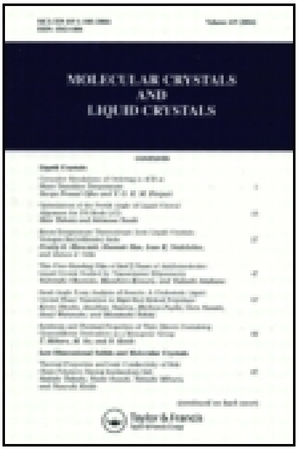

Molecular Crystals and Liquid Crystals
Publication details, including instructions for authors and subscription information:
http://www.tandfonline.com/loi/gmcl20

THERMAL PROPERTIES AND IONIC CONDUCTIVITY OF IMIDAZOLIUM SALT DERIVATIVES HAVING A CALAMITIC MESOGEN

Hideyuki Yoshizawa [a] , Takashi Mihara [a] & Naoyuki Koide* [a]

[a] Department of Chemistry, 1-3 Kagurazaka, Shinjuku-ku, Tokyo, Japan, 162-8601

Version of record first published: 02 Sep 2010

To cite this article: Hideyuki Yoshizawa, Takashi Mihara & Naoyuki Koide* (2004): THERMAL PROPERTIES AND IONIC CONDUCTIVITY OF IMIDAZOLIUM SALT DERIVATIVES HAVING A CALAMITIC MESOGEN, Molecular Crystals and Liquid Crystals, 423:1, 61-72

To link to this article: http://dx.doi.org/10.1080/15421400490502481

Mol. Cryst. Liq. Cryst., Vol. 423, pp. 61–72, 2004
Copyright © Taylor & Francis Inc.
ISSN: 1542-1406 print/1563-5287 online
DOI: 10.1080/15421400490502481

THERMAL PROPERTIES AND IONIC CONDUCTIVITY OF IMIDAZOLIUM SALT DERIVATIVES HAVING A CALAMITIC MESOGEN

*Hideyuki Yoshizawa, Takashi Mihara, and Naoyuki Koide**
Department of Chemistry, Faculty of Science, Science University of Tokyo, 1-3 Kagurazaka, Shinjuku-ku, Tokyo 162-8601, Japan

We synthesized low molar mass liquid crystals having imidazolium salt to investigate thermal properties and ionic conductivity. Two smectic (smectic A and smectic E) phases were shown for imidazolium salt derivatives, regardless of spacer length. The ionic conductivity of imidazolium salt derivatives in the smectic E phase increased with increasing temperature. The ionic conductivity of imidazolium salt derivatives was about 10^{-8}*–*10^{-7} *Scm*$^{-1}$ *near room temperature. The highest value of ionic conductivity for imidazolium salt derivatives was about* 10^{-3} *Scm*$^{-1}$ *at 140°C.*

Keywords: ionic liquid; imidazolium salt; liquid crystal

INTRODUCTION

Ionic liquids are intensively investigated based on the properties of nonvolatility, incombustibility, chemical stability, high ionic conductivity, etc. [1–6]. Imidazolium salts are especially well known as one of ionic liquids, and the physical properties of the imidazolium salts and their application to a solvent have been investigated by many researchers [7–11].

From the standpoint of low molar mass liquid crystalline (LC) compounds, ammonium salts, pyridinium salts, or imidazolium salts with a long alkyl chain would easily display a smectic phase [12–16]. The introduction of the calamitic mesogenic group into the long alkyl chain is anticipated to enhance the liquid crystallinity of the organic salts.

On the other hand, the organic salts have a possibility to be an ionic conductive material without mixing a salt as an alkali metal salt [17,18]. Gadjourova et al. reported that the ionic conductivity in the static and ordered environment of the crystalline phase of polyethylene oxide was larger that in the equivalent

*Corresponding author. E-mail: nkoide@ch.kagu.sut.ac.jp amorphous material above glass transition temperature [19]. This behavior indicated that the ionic conductivity would be expected to be favored in the static and ordered environment with permanent pathways for the ion transport. We considered that the LC state consisting of order and anisotropy would improve the conductive behavior of the ionic conductive materials.

In this report, to investigate thermal properties and ionic conductivity of the organic salts with a calamitic mesogen we synthesized imidazolium salt derivatives having a calamitic mesogen. Thermal properties and temperature dependence of ionic conductivity for the imidazolium salt derivatives were investigated.

EXPERIMENTAL

Materials

Calamitic liquid crystals having imidazolium salt were synthesized according to Scheme 1. Intermediates in Scheme 1 were prepared according to the conventional synthetic methods of LC monomers [20]. Synthetic procedures are described below for the imidazolium salt derivatives with eight methylene chain.

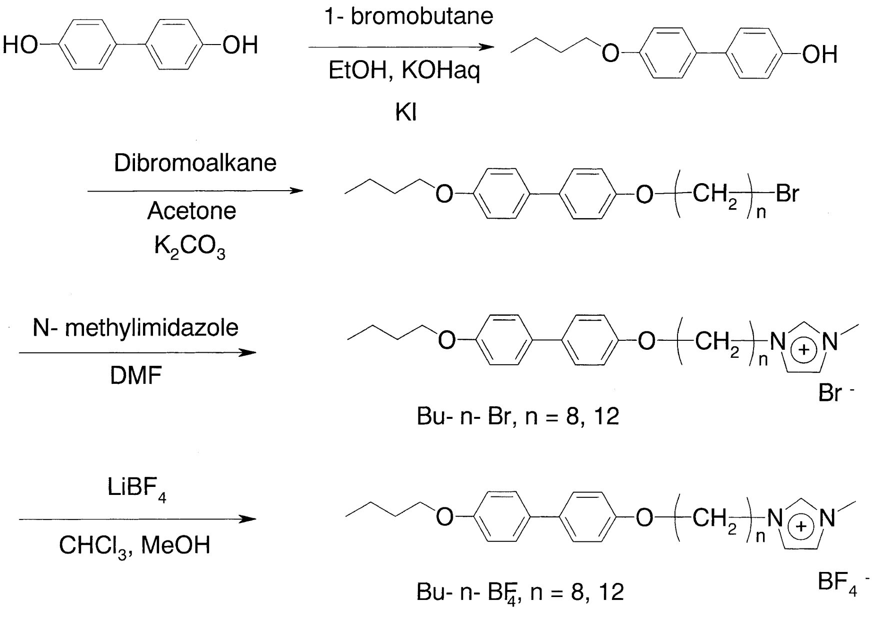

SCHEME 1 Synthesis of imidazolium salt derivatives containing a calamitic mesogen.

1-[8-(4′-Butoxy-4-biphenylyloxy)octyl]-3-methylimidazolium bromide (Bu-8-Br)

The mixture of 4-butoxy-4′-(8-bromooctyloxy)biphenyl (2.0 g, 4.6 mmol) and N-methylimidazole (2 ml, 24 mmol) was dissolved in dimethylformamide (DMF; 3 ml). After the reaction mixture was heated at 60°C for 48 h, viscous liquid was obtained. The viscous liquid was poured into diethyl ether (100 ml), and then white solid was precipitated from diethyl ether. The product was dissolved in chloroform and reprecipitated with ethyl acetate two times. The product was purified by washing with diethyl ether. The product was obtained in a 91% yield (2.2 g).

^{1}HNMR ($CDC1_3$) δ ppm: 10.44 (s, 1H, imidazolium ring), 7.41 (d, 4H, Ar), 7.37 (s, 1H, imidazolium ring), 7.28 (s, 1H, imidazolium ring), 6.90 (d, 4H, Ar), 4.28 (t, 2H, $N-CH_2$), 4.07 (s, 3H, $N-CH_3$), 3.95 (t, 2H, OCH_2), 3.93 (t, 2H, OCH_2), 0.79–1.89 (m, 19H, CH_2, CH_3).

1-[8-(4′-Butoxy-4-biphenylyloxy)octyl]-3-methylimidazolium tetrafluoroborate (Bu-8-BF_4)

A methanol solution (1 ml) of $LiBF_4$ (0.18 g, 1.9 mmol) was added dropwise to a chloroform solution (5 ml) of Bu-8-Br (1.0 g, 1.9 mmol). The reaction mixture was stirred for 3 days at room temperature. The reaction mixture was added dropwise to ethyl acetate, and then the solid was precipitated from ethyl acetate. The solid obtained was purified by washing with ethyl acetate and then with diethyl ether. The white solid was obtained in a 52.5% yield (0.53 g).

^{1}HNMR ($CDC1_3$) δ ppm: 9.68 (s, 1H, imidazolium ring), 7.37 (d, 4H, Ar), 7.18 (s, 2H, imidazolium), 6.86 (d, 4H, Ar), 4.17 (t, 2H, N–CH_2), 3.96 (s, 3H, NCH_3), 3.90 (t, 4H, OCH_2), 0.87–1.95 (m, 19H, CH_2, CH_3).

Characterization

^{1}HNMR was carried out with a JEOL JNM-LA 400 spectrometer using $CDCl_3$ as the solvent. Differential scanning calorimetry (DSC) measurements were conducted with a Mettler DSC821^e. Polarized optical microscopy measurements were performed on a Nikon polarizing optical microscope, OPTIPHOTO-POL, equipped with a Mettler FP80 controller and a FP82 hot stage. Thermal properties of imidazolium salt derivatives were investigated by polarized optical microscopy and DSC measurements. X-ray diffraction patterns were recorded with a RIGAKU RINT2500 with Ni-filtered Cu-Kα radiation. The sample in quartz capillary (diameter 1 mm) was held in a temperature-controlled cell (RIGAKU LC high-temperature controller). The ionic conductivity of the imidazolium salt derivatives was measured with alternating current (AC) impedance analyzer (Solartron Co. Impedance/Gain-Phase Analyzer SI 1260) over frequency range 10–10^6 Hz. Temperature dependence of the ionic conductivity was investigated in the temperature range between 30–150°C. The measurement temperature of the ionic conductivity was limited by the thermal stability of the polytetrafluorethylene (PTFE) tape used as a spacer for the cell. The cell used in the ionic conductivity measurements was fabricated by pressing the sample between the indium tin oxide (ITO) glass blocking electrodes with the PTFE spacer (0.25 cm^2 in a surface area of the electrode, 160 μm in the thickness of the spacer).

RESULTS AND DISCUSSION

Figure 1 shows the chemical structure of the imidazolium salt derivatives containing a calamitic mesogen. The imidazolium salt derivatives with Br anion were synthesized by addition reaction of the calamitic mesogen derivative and methylimidazole as shown in Scheme 1. On the other hand, the imidazolium salt derivatives with BF_4 anion were prepared by the exchange reaction of Br anion to BF_4 anion in the imidazolium salt derivatives. The exchange reaction of Br anion to BF_4 anion was confirmed by the shift of the peak assigned to proton of the imidazolium ring by ^{1}HNMR measurements.

Figures 2(a) and 2(b) display optical textures of Bu-12-Br at 140°C and 170°C of Bu-12-Br, respectively. Generally, ionic liquid crystals are often aligned vertically on glass substrate. Homeotropic alignment of the imidazolium salt derivatives was detected by conoscopic observation of polarized optical microscopy measurements. To obtain homogeneous alignment of the imidazolium salt derivatives, we used the glass substrate coated with the polyimide film for the observation of optical textures as shown in Figure 2. The optical textures of Bu-12-Br at 140 and 170°C support the fact that the structure of the mesophase at each temperature would be a highly ordered smectic phase and a smectic A phase, respectively. The focal conic texture of Bu-12-Br disappears above 180°C, corresponding to the clearing temperature of Bu-12-Br. Figures 2(c) and 2(d) show the optical

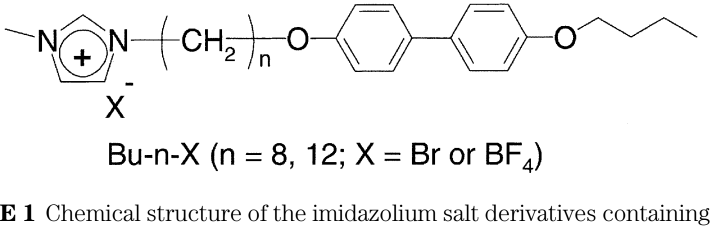

FIGURE 1 Chemical structure of the imidazolium salt derivatives containing a calamitic mesogen.

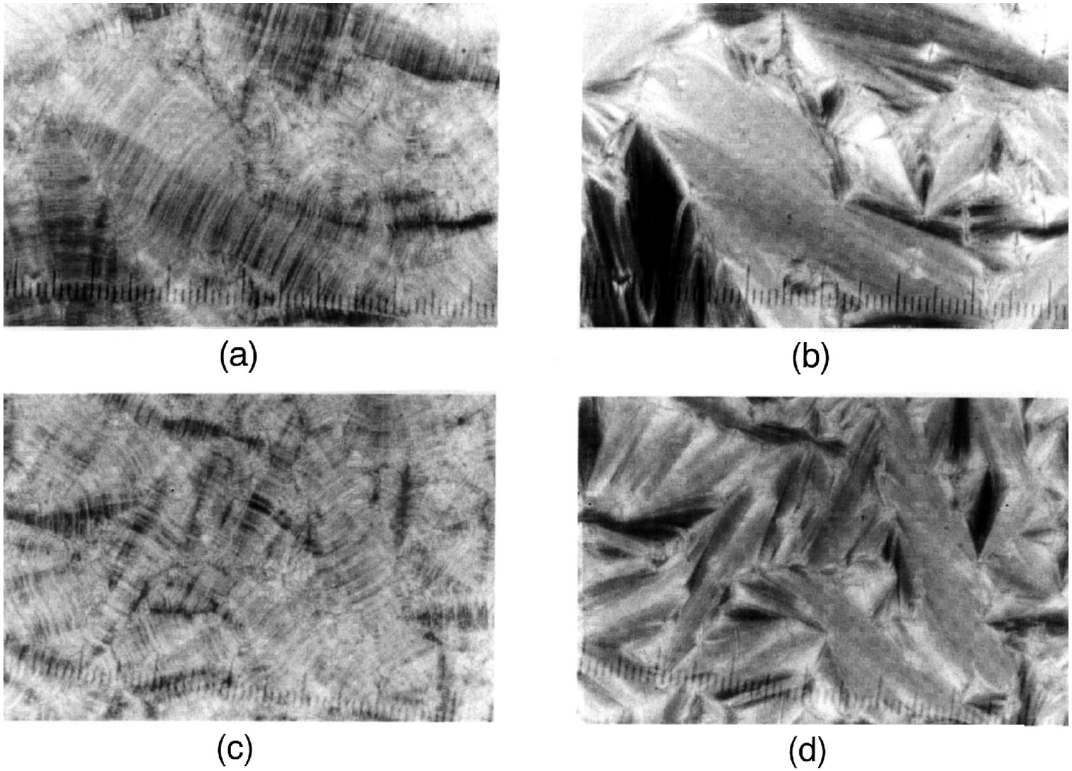

FIGURE 2 Optical textures of imidazolium salt derivative: (a) Bu-12-Br at 140°C, (b) Bu-12-Br at 170°C, (c) Bu-12-BF_4 at 145°C, and (d) Bu-12-BF_4 at 160°C.

textures of Bu-12-BF_4 at 145 and 160°C, respectively. The optical textures of Bu-12-BF_4 are similar to those of Bu-12-Br. Bu-12-BF_4 would exhibit the same mesomorphic structures as Bu-12-Br. Optical textures similar to those of Bu-12-X are also observed for Bu-8-X.

Three phase transition temperatures, including glass transition temperature, are observed in the DSC curve of Bu-12-Br. Each phase transition enthalpy changes (ΔHs) of the peaks near 154 and 180°C are 8.8 and 9.0 kJ mol^{-1}, respectively. ΔH of the peak at the clearing point of Bu-12-Br is almost the same as that of the mesophase–mesophase transition peak at 154°C. The DSC curve of Bu-8-Br is similar to that Bu-12-Br. Phase transition temperatures (138 and 156°C) of Bu-8-Br are lower than those of Bu-12-Br. ΔHs of the peaks at 138 and 156°C are 12.7 and 3.8 kJ mol^{-1}, respectively. The phase transition temperatures and phase transition enthalpy changes of the imidazolium salt derivatives would be influenced by the length of the flexible spacer.

Figure 3(a) shows the X-ray diffraction pattern of Bu-12-Br at 140°C on heating scan. A sharp peak is observed in the small-angle region of the

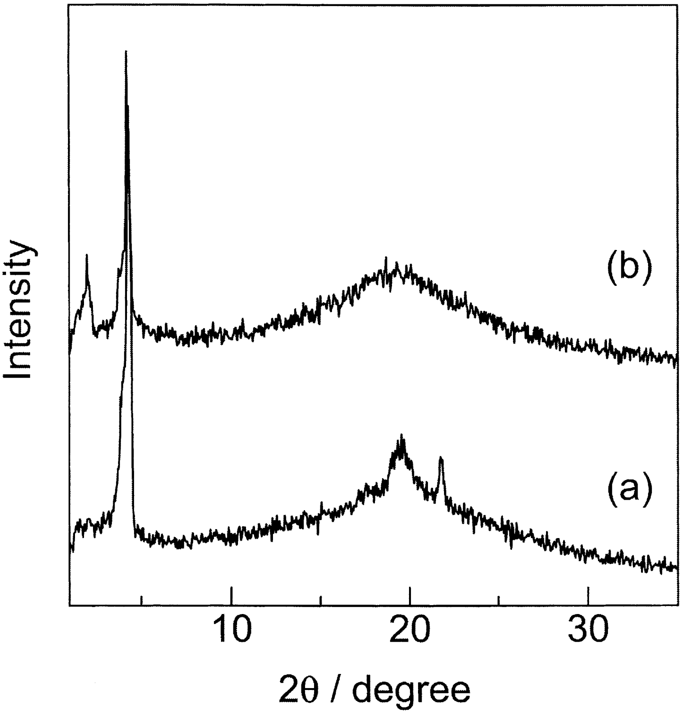

FIGURE 3 X-ray patterns of Bu-12-Br at (a) 140°C and (b) 170°C.

X-ray diffraction pattern. The d-spacing based upon the sharp peak is 21.3 Å. On the other hand, two peaks are observed in the wide-angle region. The d-spacings of the two peaks in the wide-angle region are 4.5 and 4.0 Å, respectively. The calculated length of Bu-12-Br with all-trans conformation is 34.8 Å. The d-spacing based upon the peak in the small-angle region of Bu-12-Br is shorter than the calculated molecular length. Therefore, the smectic layer would consist of a tilted or interdigitated structure formed by the mesogens. However at the present time, details of the diffraction peak near 4.2° are not clarified. The appearance of the two peaks in the wide-angle region indicates the highly ordered packing of the molecules in the smectic layer as shown in a smectic E phase.

Figure 3(b) shows the X-ray diffraction pattern of Bu-12-Br at 170°C on heating scan. Two sharp peaks are observed in the small-angle region and a broad peak in the wide-angle region of the X-ray diffraction pattern. The d-spacings based on the two sharp peaks in the small-angle region are 44.1 and 20.8 Å, respectively. Therefore, the phase structure of the mesophase in the higher mesomorphic temperature range of Bu-12-Br would be a smectic A_d phase because of the d-spacing (44.1 Å) and the observation of the focal conic texture, as shown in Figure 2(b). The d-spacing (20.8 Å) due to the sharp peak near 4.3° would relate to the length between the mesogenic group and the imidazolium group. However, at the present time details of the diffraction peak near 4.3° are not clarified.

X-ray diffraction patterns of other imidazolium salt derivatives are similar to those of Bu-12-Br. Layer spacings of the imidazolium salt derivatives are summarized in Table I. According to the same consideration as that of the X-ray diffraction pattern for Bu-12-Br, we determined the structure of

TABLE I Layer Spacings of Imidazolium Salt Derivatives

			Layer spacing[c]	
Abbreviation	L/Å[a]	T/°C[b]	d_E/Å	d_A/Å
Bu-8-Br	29.8	120	17.5, 15.4	—
		150	—	45.3, 17.8
Bu-12-Br	34.8	140	21.3	—
		170	—	44.1, 20.8
Bu-8-BF_4	29.8	135	16.2	—
		140	—	36.0, 18.2, 16.1, 8.1
Bu-12-BF_4	34.8	100	20.3	—
		160	—	38.4, 19.8

[a] Molecular length in the all-trans conformation.

[b] Measurement temperature.

[c] d_E, layer spacing of smectic E phase; d_A, layer spacing of smectic A phase.

the mesophase for other imidazolium salt derivatives. The d-spacing of the imidazolium salt derivatives in the smectic A_d phase was larger than that in the smectic E phase. This result indicates that the imidazolium salt derivatives in the smectic A_d phase would form the layer structure with a longer layer spacing compared to that in the smectic E phase. Four layer spacings were observed for Bu-8-BF_4 at 140°C. The four layer spacings of Bu-8-BF_4 included two spacings concerning the second diffraction peaks. The layer spacing of imidazolium salt derivatives, except Bu-n-Br in the smectic A_d phase, increased with increasing spacer length. On the other hand, the opposite tendency concerning the layer spacing was observed for Bu-n-Br in the smectic A_d phase (Bu-8-Br: 45.3 Å and Bu-12-Br: 44.1 Å). The d-spacing of Bu-n-Br in the smectic A_d phase was longer than that of Bu-n-BF_4. However, at the present time we cannot clarify the reasons why the opposite tendency concerning the layer spacing was observed for

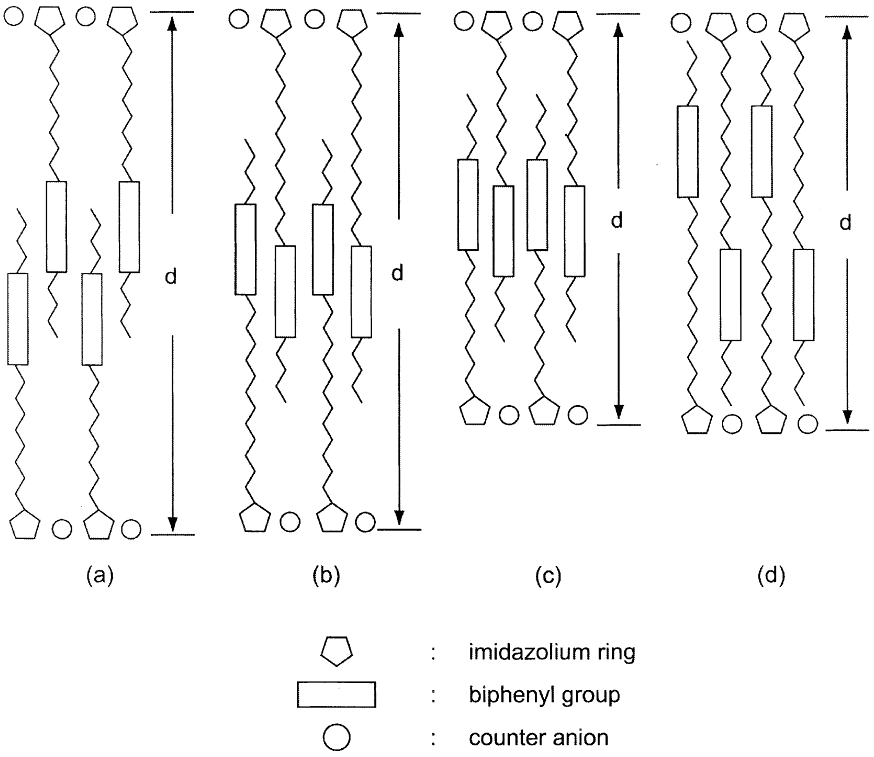

FIGURE 4 Schematic models of interdigitated structure for the imidazolium salt derivatives in each smectic A phase: (a) Bu-8-Br, (b) Bu-12-Br, (c) Bu-8-BF_4, and (d) Bu-12-BF_4.

TABLE II Phase Transition Temperature of Imidazolium Salt Derivatives with Br Anion

Abbreviation	Phase transition temperatures/°C
Bu-8-Br	$\mathrm{g} \underset{27}{\overset{29}{\rightleftarrows}} \mathrm{SmE} \underset{136(13.0)}{\overset{138(12.7)}{\rightleftarrows}} \mathrm{SmA} \underset{155(3.9)}{\overset{156(3.8)}{\rightleftarrows}} \mathrm{I}$
Bu-12-Br	$\mathrm{g} \underset{34}{\overset{38}{\rightleftarrows}} \mathrm{SmE} \underset{153(8.9)}{\overset{154(8.8)}{\rightleftarrows}} \mathrm{SmA} \underset{179(9.1)}{\overset{180(9.0)}{\rightleftarrows}} \mathrm{I}$

g, glassy; SmE, smectic E phase; SmA, smectic A phase; I, isotropic phase. Phase transition enthalpies (kJ mol^{-1}) are given in parentheses.

Bu-n-Br in the smectic A_d phase and why the d-spacing of Bu-n-Br in the smectic A_d phase was longer than that of Bu-n-BF_4.

Figure 4 demonstrates schematic models of interdigitated structure for the imidazolium salt derivatives in each smectic A phase. The interdigitated structure of the imidazolium salt derivatives in the smectic A phase would be dependent upon the spacer length and the counter anion. In the models of Bu-12-Br and Bu-8-BF_4, butoxybiphenyl groups are facing each other in the lateral direction.

Thermal properties of the imidazolium salt derivatives are summarized in Tables II and III. No mesophases are observed for the calamitic mesogen derivatives without the imidazolium salt, while imidazolium salt derivatives easily exhibit smectic phases. The appearance of smectic phases for the imidazolium salt derivatives originates from the ionic interaction between imidazolium salts. The imidazolium salt derivatives with relatively longer flexible spacer (Bu-8-X and Bu-12-X (X = Br or BF_4)) tends to display

TABLE III Phase Transition Temperatures of Imidazolium Salt Derivatives with BF_4 Anion

Abbreviation	Phase transition temperatures/°C
Bu-8-BF_4	$\mathrm{g} \underset{18}{\overset{19}{\rightleftarrows}} \mathrm{SmE} \xrightarrow{141\ (20.3)} \mathrm{I}$ $\mathrm{SmE} \xleftarrow[139\ (15.3)]{} \mathrm{SmA} \xleftarrow[141\ (5.6)]{} \mathrm{I}$
Bu-12-BF_4	$\mathrm{g} \underset{38}{\overset{39}{\rightleftarrows}} \mathrm{SmE} \underset{148\ (8.9)}{\overset{149\ (8.7)}{\rightleftarrows}} \mathrm{SmA} \underset{170\ (9.5)}{\overset{171\ (9.3)}{\rightleftarrows}} \mathrm{I}$

g, glassy; SmE, smectic E phase; SmA; smectic A phase; I, isotropic phase. Phase transition enthalpies (kJmol^{-1}) are given in parentheses.

two smectic phases. Mesomorphic temperature range for Bu-12-X is wider than that of Bu-8-X. The length of methylene spacer plays an important role for the stabilization of the smectic phases for Bu-8-X and Bu-12-X.

Mesomorphic temperature range for Bu-n-Br is slightly wider than that of Bu-n-BF_4. The difference of the mesomorphic temperature range originates from the difference in the counter anion for the imidazolium salt derivatives. The ionic interaction between imidazolium salts for Bu-n-Br is stronger than that for Bu-n-BF_4, although the size of counter anions between Br and BF_4 was not so different. The crystallization is not observed for both Bu-8-X and Bu-12-X at room temperature. A glassy state is characteristic of polymeric materials; however, the glassy state is observed for the low molar mass imidazolium salt derivatives.

Bradley et al. reported the thermal properties of the 1-alkyl-3 methylimidazolium salt [16]. 1-Dodecyl-3-methylimidazolium salt with Br anion displays a smectic A phase in the temperature range between -5.3 and 82.0°C. On the other hand, Bu-12-Br displays two smectic phases. The mesomorphic temperature range of Bu-12-Br is wider than that of 1-dodecyl-3-methylimidazolium salt with Br anion, although the temperature range of the smectic A phase for Bu-12-Br is narrower than that of the smectic A phase of 1-dodecyl-3-methylimidazolium salt with Br. The highly ordered smectic phase is induced by the introduction of butoxy biphenyl group into the alkyl chain.

The exhibition of the highly ordered smectic phase (smectic E phase) for the resulting imidazolium salt derivatives would arise from some factors such as van der Waals force of the butoxybiphenyl groups. However, details of the reason why the introduction of the butoxybiphenyl group into the alkyl chain leads to the exhibition of the smectic E phase for the resulting imidazolium salt derivative are not clarified at the present time.

Holbrey et al. also reported the thermal properties of 1-dodecyl-3-methylimidazolium salt with BF_4 anion [15]. 1-Alkyl-3-methylimidazolium salt with BF_4 also displayed a smectic A phase in the temperature range between 26.4 and 38.5°C. The mesomorphic temperature range of Bu-12-BF_4 is also larger than that of 1-dodecyl-3-methylimidazolium salt with BF_4 anion. The smectic phase of Bu-12-BF_4 is stabilized by the introduction of butoxybiphenyl group into 1-dodecyl-3-methylimidazolium salt with BF_4 anion.

Figure 5(a) shows temperature dependence of the ionic conductivity for the imidazolium salt derivatives with Br anion. In this study, we measured the ionic conductivity for the imidazolium salt derivatives only in smectic E phase, owing to the limit of thermal stability of the PTFE tape used as a spacer for the cell. The ionic conductivity of Bu-8-Br and Bu-12-Br increases with increasing temperature. The value of the ionic conductivity for Bu-12-Br increases rapidly near the phase transition temperature from

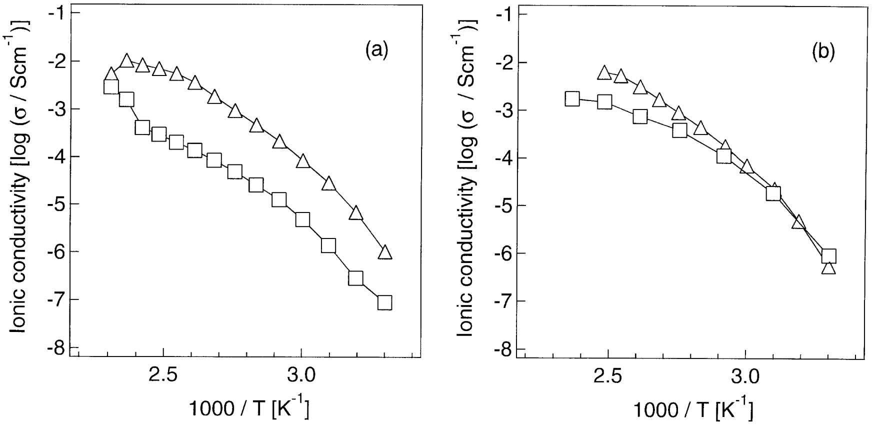

FIGURE 5 Temperature dependence of ionic conductivity of (a) Bu-n-Br and (b) Bu-n-BF_4: open triangles, n = 8; open squares, n = 12.

highly ordered smectic phase to smectic A phase. The value of the ionic conductivity for Bu-8-Br is larger than that of Bu-12-Br in the measurement temperature range. Figure 5(b) also displays temperature dependence of the ionic conductivity for Bu-n-BF_4. The value of the ionic conductivity for Bu-n-BF_4 increases with increasing temperature. The value of the ionic conductivity for Bu-8-BF_4 is larger than that of Bu-12-BF_4. The value of the ionic conductivity for Bu-8-X is larger than that of Bu-12-X. This behavior concerning the ionic conductivity indicates that a too-long methylene spacer would depress the ion conduction in the imidazolium salt derivative.

The difference in length of the methylene spacer would lead to the difference in the hydrophobicity of the imidazolium salt derivative. The hydrophobicity of Bu-12-X would be larger than that of Bu-8-X. The effect of the hydrophobicity on the reduction of the ionic conductivity in the imidazolium salt derivatives would be dependent upon the anion (Br anion or BF_4 anion). The magnitude of the reduction of ionic conductivity for the imidazolium salt derivatives with Br anion would be larger than that with BF_4 anion, as shown in Figure 5(a). However, details of the difference in the ionic conductive behavior for the imidazolium salt derivatives are not clarified at the present time.

To investigate anisotropy of the ionic conductivity for the imidazolium salt derivatives, we tried to obtain the sample with the homogeneous alignment by imposing shear stress. However, we cannot obtain the sample with the stable homogeneous alignment at the present time. The homogeneous alignment of the imidazolium salt derivatives is not stable against the change of temperature and annealing. Immediately after imposing shear stress on the sample, we obtained the homogeneous alignment of the imidazolium salt derivatives. We could confirm the initial homogeneous alignment of the imidazolium salt derivatives in the cell after imposing shear stress. However, partially homeotropic alignment of the imidazolium salt derivatives was induced by the annealing or the temperature change. Therefore, at the present time we cannot clarify the anisotropy of ionic conductivity by measuring the ionic conductivity for the imidazolium salt derivatives with homogeneous alignment and with homeotropic alignment.

REFERENCES

[1] Welton, T. (1999). *Chem. Rev.*, *99*, 2071–2083.

[2] Huddleston, J. G., Willauer, H. D., Swatloski, R. P., Visser, A. E., & Rogers, R. D. (1998). *Chem. Commun.*, 1765–1766.

[3] Koch, V. R., Nanjundiah, C., Appetecchi, G. B., & Scrosati, B. (1995). *J. Electrochem. Soc.*, *142*, L116–L118.

[4] Papageorgiou, N., Athanassov, Y., Armand, M., Bonhôte, P., Pettersson, H., Azam, A., & Grätzel, M. (1996). *J. Electrochem. Soc.*, *143*, 3099–3108.

[5] Matsumoto, H., Matsuda, T., Tsuda, T., Hagiwara, R., Ito, Y., & Miyazaki, Y. (2001). *Chem. Lett.*, 26–27.

[6] Doyle, M., Choi, S. K., & Proulx, G. (2000). *J. Electrochem. Soc.*, *147*, 34–37.

[7] Bonhôte, P., Dias, A.-P., Papageorgiou, N., Kalyanasundaram, K., & Grätzel, M. (1996). *Inorg. Chem.*, *35*, 1168–1178.

[8] MacFarlane, D. R., Huang, J., & Forsyth, M. (1999). *Nature*, *402*, 792–794.

[9] MacFarlane, D. R., Sun, J., Golding, J., Meakin, P., & Forsyth, M. (2000). *Electrochim. Acta.*, *45*, 1271–1278.

[10] Hagiwara, R. (2002). *Electrochemistry*, *70*, 130–136.

[11] Olivier-Bourbigou, H. & Magna, L. (2002). *J. Mol. Catal. A*, *182–183*, 419–437.

[12] Navarro-Rodriguez, D., Frere, Y., Gramain, P., Guillon, D., & Skoulios, A. (1991). *Liq. Cryst.*, *9*, 321–335.

[13] Bowlas, C. J., Bruce, D. W., & Seddon, K. R. (1996). *Chem. Commun.*, 1625–1626.

[14] Lee, K. M., Lee, C. K., & Lin, I. J. B. (1997). *Chem. Commun.*, 899–900.

[15] Holbrey, J. D. & Seddon, K. R. (1999). *J. Chem. Soc., Dalton Trans.*, 2133–2139.

[16] Bradley, A. E., Hardacre, C., Holbrey, J. D., Johnston, S., McMath, S. E. J., & Nieuwenhuyzen, N. (2002). *Chem. Mater.*, *14*, 629–635.

[17] Yoshio, M., Mukai, T., Kanie, K., Yoshizawa, M., Ohno, H., & Kato, T. (2002). *Chem. Lett.*, 320–321.

[18] Yoshio, M., Mukai, T., Kanie, K., Yoshizawa, M., Ohno, H., & Kato, T. (2002). *Adv. Mater.*, *14*, 351–354.

[19] Gadjourova, Z., Andreev, Y. G., Tunstall, D. P., & Bruce, P. G. (2001). *Nature*, *412*, 520–523.

[20] McArdle, C. B. (Ed.) (1989). *Side chain liquid crystal polymers*, Blackie: Glasgow and Chapman and Hall: New York.